

Discrete-time thermodynamic speed limit

Sangyun Lee,^{1,2} Jae Sung Lee,^{2,*} and Jong-Min Park^{3,4,†}

¹*Institute for Physical Science and Technology, University of Maryland, College Park, Maryland 20742, USA*

²*School of Physics, Korea Institute for Advanced Study, Seoul, 02455, Korea*

³*Asia Pacific Center for Theoretical Physics, Pohang 37673, Korea*

⁴*Department of Physics, POSTECH, Pohang 37673, Korea*

As a fundamental thermodynamic principle, speed limits reveal the lower bound of entropy production (EP) required for a system to transition from a given initial state to a final state. While various speed limits have been developed for continuous-time Markov processes, their application to discrete-time Markov chains remains unexplored. In this study, we investigate the speed limits in discrete-time Markov chains, focusing on two types of EP commonly used to measure the irreversibility of a discrete-time process: time-reversed EP and time-backward EP. We find that time-reversed EP satisfies the speed limit for the continuous-time Markov processes, whereas time-backward EP does not. Additionally, for time-reversed EP, we derive practical speed limits applicable to systems driven by cyclic protocols or with unidirectional transitions, where conventional speed limits become meaningless or invalid. We show that these relations also hold for continuous-time Markov processes by taking the time-continuum limit of our results. Finally, we validate our findings through several examples.

I. INTRODUCTION

Entropy production (EP) is a central thermodynamic quantity that reveals the irreversibility inherent in non-equilibrium processes. The mathematical formulation of EP for microscopic stochastic processes has been developed within the framework of stochastic thermodynamics [1, 2], leading to the discovery of invaluable thermodynamic relations. The representative one is fluctuation theorems [1, 3–8], which are expressed as equalities, offering more detailed information about EP compared to the second law of thermodynamics. They represent fundamental symmetries in the distributions of thermodynamic quantities and provide experimental methods to measure the free energy difference between two states from nonequilibrium processes [3, 4, 9].

In addition to the fluctuation theorems, numerous thermodynamic tradeoff relations have been discovered, surpassing the bound of the second law. These include the thermodynamic uncertainty relation (TUR) [10–20], entropic bounds [21], and fluctuation-response inequalities [22]. These relations establish non-trivial lower bounds on EP in terms of generic non-equilibrium currents. They are instrumental in deriving power-efficiency tradeoff relations [23–26] and bounds on the turnover time scale of anomalous diffusions [27]. Moreover, these relations enable the inference of EP from experimental data without necessitating knowledge of the governing equations [28–32].

Another important finding is the discovery of thermodynamic speed limits. It establishes a bound on EP in terms of probability distance and the dynamical activity [16, 33–38]. Recently, the speed limit

has been utilized to derive the finite-time Landauer’s bound [34, 35, 38, 39], while also interpreting it as part of a unified hierarchical tradeoff relations [40]. Previous studies on speed limits [41] have focused on continuous-time Markov processes, where transition times are continuous. However, various interesting phenomena occur in discrete-time setups, such as Monte Carlo simulations, financial and stock price, Page Rank algorithm, and biochemical dynamics [42]. Despite their prevalence, the study of speed limits in discrete-time settings remains unexplored. Regarding the TURs, the conventional TUR derived for continuous-time Markov processes is violated in discrete-time processes, leading to a modification of the TUR formulation [11, 14, 43, 44]. In this context, it is intriguing and important to investigate the effects of time discretization on speed limits.

Here, we study speed limits for discrete-time Markov chains. For discrete-time processes, there are two widely accepted EP formulations: time-reversed EP and time-backward EP [14, 39, 45–47], which converge to the same value in continuous-time the limit. We investigate speed limits for these EPs and verify that the speed limit derived for continuous-time Markov processes still holds for time-reversed EP, while it is violated for time-backward EP. We quantify the degree of this violation using the Kullback-Leibler divergence between consecutive probability distributions. This indicates that the bound of the speed limit depends on the choice of EP formulation and that modification from the conventional form is required for time-backward EP. We also find the saturation conditions of the speed limits for time-reversed EP. In addition, we present practical speed limits for processes with unidirectional transitions or cyclic steady states, where conventional speed limits become invalid or meaningless. Our results, based on discrete-time processes, can be straightforwardly extended to continuous-time processes by taking their continuous-time limits. We also validate our findings through numerical calculations.

* jslee@kias.re.kr

† jongmin.park@apctp.org

This article is organized as follows. In Sec. II, we review the two formulations of EP for a discrete-time Markov chain. In Sec. III, we present the derivation of speed limits for these EPs in discrete-time Markov chains. Specifically, we derive the stepwise speed limit, which requires the full information of probability distributions at all time steps, and the section speed limit, which necessitates only partial information on probability distributions at limited time steps. The saturation condition for the speed limits is also discussed. In Sec. IV, we extend our result to a Markov chain with unidirectional transitions. In Sec. V, we numerically verify our results through three examples. Finally, we conclude in Sec. VI.

II. ENTROPY PRODUCTIONS

Before discussing the speed limits, we first revisit the formulations of EP for a discrete-time Markov chain. We denote the i -th transition time occurred during the process by t_i for $i = 0, 1, \dots, N$ with a time gap $\Delta t = t_{i+1} - t_i$ and the probability of state n at time t_i by $P_n(t_i)$. The Markov chain is characterized by the transition probability $M_{n,m}(t_i)$, denoting the probability of transition from the state m at t_i to n at t_{i+1} . We assume that the system obeys microscopic reversibility, i.e., $M_{n,m}(t) \neq 0$ if $M_{m,n}(t) \neq 0$. The case involving unidirectional transitions will be discussed in Sec. IV. In terms of $P_n(t_i)$ and $M_{n,m}(t_i)$, probability of state n at t_{i+1} is determined by the following equation:

$$P_n(t_{i+1}) = \sum_m M_{n,m}(t_i) P_m(t_i). \quad (1)$$

Using the normalization condition of the transition probability, $\sum_n M_{n,m}(t_i) = 1$, this equation can be rearranged as

$$\begin{aligned} P_n(t_{i+1}) - P_n(t_i) \\ = \sum_{m(\neq n)} [M_{n,m}(t_i) P_m(t_i) - M_{m,n}(t_i) P_n(t_i)]. \end{aligned} \quad (2)$$

This equation is analogous to the following master equation for a continuous-time Markov process:

$$\dot{P}_n(t) = \sum_{m(\neq n)} [R_{n,m}(t) P_m(t) - R_{m,n}(t) P_n(t)], \quad (3)$$

where $R_{n,m}(t)$ is the transition rate at time t . EP rate for this continuous-time Markov process is given as [2]

$$\dot{\Sigma}_{\text{cont}}(t) = \sum_{n,m} R_{n,m}(t) P_m(t) \ln \frac{R_{n,m}(t) P_m(t)}{R_{m,n}(t) P_n(t)}. \quad (4)$$

From Eq. (4), two formulations of EP for a discrete-time Markov chain can be deduced: (i) time-reversed EP $\tilde{\Sigma}$ [14, 47] and (ii) time-backward EP Σ [39, 46].

Integrating Eq. (4) over the infinitesimal time interval $dt = t_{i+1} - t_i$ leads to

$$\Delta \Sigma_{\text{cont}} = \int_{t_i}^{t_{i+1}} dt' \sum_{n,m} R_{n,m}(t') P_m(t') \ln \frac{R_{n,m}(t') P_m(t')}{R_{m,n}(t') P_n(t')} \quad (5)$$

$$= \Delta S_{\text{sys}}(t_i) + \int_{t_i}^{t_{i+1}} dt' \sum_{n,m} R_{n,m}(t') P_m(t') \ln \frac{R_{n,m}(t')}{R_{m,n}(t')}, \quad (6)$$

where the system entropy change is defined as $\Delta S_{\text{sys}}(t_i) \equiv \sum_n [P_n(t_i) \ln P_n(t_i) - P_n(t_{i+1}) \ln P_n(t_{i+1})]$. Equation (3) is used to obtain Eq. (6) from Eq. (5). For an infinitesimal dt , Eq. (5) can be approximated as

$$\begin{aligned} \Delta \Sigma_{\text{cont}} &\approx \sum_{n,m} R_{n,m}(t_i) dt P_m(t_i) \ln \frac{R_{n,m}(t_i) P_m(t_i)}{R_{m,n}(t_i) P_n(t_i)} \\ &= \sum_{n,m} M_{n,m}(t_i) P_m(t_i) \ln \frac{M_{n,m}(t_i) P_m(t_i)}{M_{m,n}(t_i) P_n(t_i)} \equiv \Delta \tilde{\Sigma}(t_i), \end{aligned} \quad (7)$$

where we used the relation $M_{n,m}(t_i) = \delta_{n,m} + R_{n,m}(t_i) dt + O(dt^2)$. The formulation $\Delta \tilde{\Sigma}(t_i)$ in Eq. (7) represents EP generated during one discrete-time step and has been used as a measure of irreversibility or EP in discrete-time processes. This EP is referred to as time-reversed EP. Note that the probabilities P_m and P_n in $\Delta \tilde{\Sigma}(t_i)$ depend solely on a single time t_i , and thus, time-reversed EP shares the same mathematical form as the EP rate for continuous-time processes in Eq. (4). It is also interesting to note that the diagonal terms with $n = m$ in Eq. (7) do not contribute to $\Delta \tilde{\Sigma}(t_i)$ as in continuous-time EP rate $\dot{\Sigma}_{\text{cont}}(t)$.

Alternatively, starting from Eq. (6), one can derive another formulation of EP for discrete-time processes. Using the normalization condition $\sum_n M_{n,m}(t_i) = 1$ and Eq. (1), we can show

$$\begin{aligned} \sum_{n,m} M_{n,m}(t_i) P_m(t_i) \ln \frac{P_m(t_i)}{P_n(t_{i+1})} \\ = \sum_n P_n(t_i) \ln P_n(t_i) - \sum_n P_n(t_{i+1}) \ln P_n(t_{i+1}) \end{aligned} \quad (8)$$

which is identical to $\Delta S_{\text{sys}}(t_i)$. Plugging Eq. (8) into Eq. (6), we arrive at

$$\begin{aligned} \Delta \Sigma_{\text{cont}} &\approx \Delta S_{\text{sys}}(t_i) + \sum_{n,m} R_{n,m}(t_i) dt P_m(t_i) \ln \frac{R_{n,m}(t_i)}{R_{m,n}(t_i)} \\ &= \sum_{n,m} M_{n,m}(t_i) P_m(t_i) \ln \frac{M_{n,m}(t_i) P_m(t_i)}{M_{m,n}(t_i) P_n(t_{i+1})} \equiv \Delta \Sigma(t_i). \end{aligned} \quad (9)$$

This formulation, $\Delta \Sigma(t_i)$, is called time-backward EP. Different from time-reversed EP, $\Delta \Sigma(t_i)$ necessitates the

information of the next-time probability $P_n(t_{i+1})$ as well as current-time one $P_n(t_i)$. The first line of Eq. (9) displays the decomposition of time-backward EP into the system entropy change and the contribution of the environment. In this context, time-backward EP is often employed in the studies related to thermodynamics. Unlike time-reversed EP, time-backward EP depends on the staying probability, meaning that events where the system remains in the same state also contribute to time-backward EP.

By using the log inequality $\ln(1/x) \geq 1 - x$ for $x > 0$, one can show that both EPs are always non-negative regardless of the magnitude of the time interval. In addition, $\Delta\tilde{\Sigma} \geq \Delta\Sigma$ can be proved by utilizing the same log inequality as follows:

$$\Delta\Sigma'(t_i) \equiv \Delta\tilde{\Sigma}(t_i) - \Delta\Sigma(t_i) = D[\mathbf{P}(t_{i+1}) \parallel \mathbf{P}(t_i)] \geq 0, \quad (10)$$

where $D[\mathbf{p} \parallel \mathbf{q}] = \sum_n p_n \ln(p_n/q_n)$ denotes the Kullback-Leibler divergence of a probability p_n with respect to a probability q_n . In the continuous-time limit, their difference $\Delta\Sigma'$ vanishes at the order of the square of the time interval. Thus, both EPs become identical in the limit.

III. DISCRETE-TIME SPEED LIMITS

A. Stepwise speed limit

In this section, we describe the process of deriving speed limits for discrete-time systems, focusing initially on time-reversed EP $\tilde{\Sigma}$. The speed limit can be derived through the method used in previous works [34, 35], since the time-reversed EP shares the same mathematical structure as the EP rate for continuous-time processes. Thus, we can express $\Delta\tilde{\Sigma}(t_i)$ as the following Kullback-Leibler divergence form:

$$\begin{aligned} \Delta\tilde{\Sigma}(t_i) &= A(t_i) \sum_{n,m} Q_{n,m}(t_i) \ln \frac{Q_{n,m}(t_i)}{Q_{m,n}(t_i)} \\ &= A(t_i) D[\mathbf{Q}(t_i) \parallel \mathbf{Q}^T(t_i)], \end{aligned} \quad (11)$$

where $Q_{n,m}(t_i)$ is a joint probability defined as $Q_{n,m}(t_i) \equiv M_{n,m}(t_i)P_m(t_i)/A(t_i)$ with normalization condition $\sum_{n \neq m} Q_{n,m}(t_i) = 1$, $A(t_i) \equiv \sum_{n \neq m} M_{m,n}(t_i)P_n(t_i)$ is the dynamical activity, and T denotes the transpose of a matrix, i.e., $Q_{n,m}^T(t_i) = Q_{m,n}(t_i)$.

The Kullback-Leibler divergence is lower bounded by a function of the total variation distance which is a measure of the distance between two distributions, defined as $d_{\text{TV}}[\mathbf{p}, \mathbf{q}] \equiv \sum_n |p_n - q_n|/2$. This bound can be comprehensively expressed as [35]

$$D[\mathbf{Q}(t_i) \parallel \mathbf{Q}^T(t_i)] \geq h(d_{\text{TV}}[\mathbf{Q}(t_i), \mathbf{Q}^T(t_i)]), \quad (12)$$

where $h(x)$ represents a convex function satisfying Eq. (12). Several such functions have been found, for

example, $h(x) = 2x^2$ for Pinsker's inequality [48] and $h(x) = \ln[(1+x)^{-1+x}/(1-x)]$ for Gilardoni's inequality [49]. Specifically, when the Kullback-Leibler divergence satisfies the symmetry condition $D[\mathbf{p} \parallel \mathbf{q}] = D[\mathbf{q} \parallel \mathbf{p}]$, the function $h(x) = x \ln[(1+x)/(1-x)] \equiv h_{\text{sym}}(x)$ can be used and it provides the tightest bound [35]. As $D[\mathbf{Q} \parallel \mathbf{Q}^T]$ in Eq. (12) is symmetric, $h_{\text{sym}}(x)$ can be employed. It is also worth noting that every $h(x)$ is a monotonically increasing function for $x \geq 0$.

Combining Eqs. (11) and (12), we can derive the lower bound of time-reversed EP in terms of dynamical activity $A(t_i)$ and $\mathbf{Q}(t_i)$ as follows:

$$\Delta\tilde{\Sigma}(t_i) \geq A(t_i) h(d_{\text{TV}}[\mathbf{Q}(t_i), \mathbf{Q}^T(t_i)]). \quad (13)$$

As the next step, by employing the following triangle inequality

$$\begin{aligned} &\sum_{m(\neq n)} |M_{n,m}(t_i)P_m(t_i) - M_{m,n}(t_i)P_n(t_i)| \\ &\geq \left| \sum_{m(\neq n)} M_{n,m}(t_i)P_m(t_i) - M_{m,n}(t_i)P_n(t_i) \right| \end{aligned} \quad (14)$$

and Eq. (2), we can derive the lower bound of the total variation distance for $\mathbf{Q}(t_i)$ as

$$\begin{aligned} d_{\text{TV}}[\mathbf{Q}(t_i), \mathbf{Q}^T(t_i)] &= \sum_n \frac{\sum_{m(\neq n)} |Q_{n,m}(t_i) - Q_{m,n}(t_i)|}{2} \\ &\geq \sum_n \frac{|P_n(t_{i+1}) - P_n(t_i)|}{2A(t_i)} = \frac{d_{i+1,i}}{A(t_i)} \end{aligned} \quad (15)$$

where $d_{i+1,i} \equiv d_{\text{TV}}[\mathbf{P}(t_{i+1}), \mathbf{P}(t_i)]$. Plugging Eq. (15) into Eq. (13) under the monotonically increasing property of $h(x)$ and summing over all i yield

$$\tilde{\Sigma} = \sum_{i=0}^{N-1} \Delta\tilde{\Sigma}(t_i) \geq \sum_{i=0}^{N-1} A(t_i) h \left\{ \frac{d_{i+1,i}}{A(t_i)} \right\}. \quad (16)$$

We call equation (16) stepwise speed limit, as the lower bound of the entire EP is estimated by summing all time-step bounds.

By treating the bound as the average of a convex function $h(x)$ over a distribution $A(t_i)/A_{\text{tot}}$ with $A_{\text{tot}} \equiv \sum_{i=0}^{N-1} A(t_i)$, one can apply the Jensen's inequality as follows:

$$\sum_{i=0}^{N-1} \frac{A(t_i)}{A_{\text{tot}}} h \left(\frac{d_{i+1,i}}{A(t_i)} \right) \geq h \left(\sum_{i=0}^{N-1} \frac{d_{i+1,i}}{A_{\text{tot}}} \right). \quad (17)$$

Applying Eq. (17) into Eq. (16), we finally arrive at

$$\tilde{\Sigma} \geq A_{\text{tot}} h \left\{ \sum_{i=0}^{N-1} \frac{d_{i+1,i}}{A_{\text{tot}}} \right\}. \quad (18)$$

This expression is applicable when $P(t_0) = P(t_N)$ and yields a nontrivial bound for this case. We note that A_{tot} can be computed by averaging the number of transitions between all different states without the knowledge of $\mathbf{P}(t)$. On another note, a relation similar, in terms of Wasserstein distance, to Eq. (18) for continuous-time processes was reported in Ref. [41].

B. Section speed limit

To evaluate the bound of the stepwise speed limit (18), full information on $\mathbf{P}(t)$ at all time steps is required. However, acquiring all the information on the temporal evolution of $\mathbf{P}(t)$ is not always possible. There may be cases where partial information on $\mathbf{P}(t)$ at limited time steps is available. Hence, it would be useful to find alternative bounds utilizing less information on $\mathbf{P}(t)$. Here, we present a speed limit using the knowledge of probability distributions only at two time points. To this end, we employ the triangle inequality for the total variation distance as follows:

$$\sum_{i=0}^{N-1} d_{i+1,i} \geq d_{\text{TV}}[\mathbf{P}(t_{\text{F}}), \mathbf{P}(t_{\text{I}})] \quad (19)$$

for any intermediate times t_{I} and t_{F} within $[t_0, t_N]$. Then, from the monotonically increasing property of $h(x)$, the stepwise speed limit (18) can be simplified as

$$\tilde{\Sigma} \geq A_{\text{tot}} h \left(\frac{d_{\text{TV}}[\mathbf{P}(t_{\text{F}}), \mathbf{P}(t_{\text{I}})]}{A_{\text{tot}}} \right). \quad (20)$$

We call Eq. (20) section speed limit. By introducing a function $g(x) \equiv h(x)/(2x)$, one can rearrange Eq. (20) in the following conventional form of a speed limit:

$$t_N \geq \frac{d_{\text{TV}}[\mathbf{P}(t_{\text{F}}), \mathbf{P}(t_{\text{I}})]}{\bar{A} g^{-1} \left(\frac{\tilde{\Sigma}}{2d_{\text{TV}}[\mathbf{P}(t_{\text{F}}), \mathbf{P}(t_{\text{I}})]} \right)}, \quad (21)$$

where $\bar{A} = A_{\text{tot}}/t_N$. When we set $t_{\text{I}} = t_0$ and $t_{\text{F}} = t_N$, Eq. (21) has the same mathematical form as the continuous-time speed limit [18, 34].

It is worth comparing the EP bound derived from our results with the TUR for discrete-time Markov chains. The EP lower bound of the discrete-time TUR is exponentially suppressed [43] or proportional to the minimum staying probability [14]. Moreover, the discrete-time TUR applies only to systems without time-dependent driving, whereas our speed limit has no such constraint. This highlights the potential utility of our result for estimating EP in discrete-time processes with arbitrary driving protocols.

In addition, the section speed limit can yield a nontrivial bound for cyclic processes, whereas the conventional speed limit becomes trivial due to the complete cycle condition $\mathbf{P}(t_0) = \mathbf{P}(t_N)$ in a cyclic process. We present a concrete application of the section speed limit on a cyclic steady state in Sec. V.

From Eq. (10), the speed limit for the time-backward EP can be obtained using

$$\Sigma \geq A_{\text{tot}} h \left(\frac{d_{\text{TV}}[\mathbf{P}(t_{\text{F}}), \mathbf{P}(t_{\text{I}})]}{A_{\text{tot}}} \right) - \sum_{i=0}^{N-1} \Delta \Sigma'(t_i). \quad (22)$$

Evaluating the last term on the right-hand side requires information about distributions at all time steps. Furthermore, the lower bound of the time-backward EP is smaller than that of the time-reversed EP, indicating that the time-backward EP violates the conventional speed limit. In Sec. V A, we will demonstrate an example of this violation in a simple two-state system.

C. Saturation condition

We now investigate the condition for each speed limit being saturated. They saturate when the equality conditions for all inequalities used to derive each speed limit are satisfied. In this regard, inequalities (12) and (14) are used to derive the stepwise speed limit, and additional inequalities (17) and (19) are applied for the section speed limit. First, the equality condition of Eq. (14) is satisfied when the system has only two states. Interestingly, for a two-state system, Eq. (12) also saturates regardless of the protocol $M_{nm}(t)$ when we adopt $h_{\text{sym}}(x) = x \ln[(1+x)/(1-x)]$. Therefore, the stepwise speed limit always saturates for any two-state system. The equal sign of Eq. (17) is attainable when the following condition is satisfied:

$$\frac{d_{i+1,i}}{A(t_i)} = \frac{d_{j+1,j}}{A(t_j)} \quad (23)$$

for any $i \neq j$. Finding the general saturation condition for inequality (19) is difficult. Nonetheless, the equality of Eq. (19) is attainable when the process ends after only a single time step, i.e., $N = 1$, as the section speed limit and stepwise speed limit become identical when $N = 1$.

In short, regardless of the protocol $M_{n,m}(t_i)$, the equality of the stepwise speed limit is achieved for two-state systems with any number of time steps, and the section speed limit saturates in one-time step processes of a system with only two states.

IV. SPEED LIMIT WITH UNIDIRECTIONAL TRANSITIONS

We now extend our results to systems that include both bidirectional and unidirectional transitions. A bidirectional transition refers to a transition where the corresponding backward transition exists, while a unidirectional transition refers to a transition where the backward transition is absent. We use a superscript $\alpha = \text{u}$ or b to represent the transition probability associated with the bidirectional or unidirectional transition, respectively. That is, $M_{n,m}^{(\text{u})}(t_i)$ and $M_{n,m}^{(\text{b})}(t_i)$ denote that

the transition from m state to n state is unidirectional and bidirectional, respectively. Therefore, if $M_{n,m}^{(u)}(t_i)$ is nonzero, $M_{m,n}^{(u)}(t_i)$ must be 0. Conversely, if $M_{n,m}^{(b)}(t_i)$ is nonzero, $M_{m,n}^{(b)}(t_i)$ must also be nonzero. With this notation, the equation of motion can be written as

$$P_n(t_{i+1}) = \sum_{\alpha=u,b} \sum_m^{(\alpha)} M_{n,m}^{(\alpha)}(t_i) P_m(t_i), \quad (24)$$

where $\sum_m^{(\alpha)}$ denotes summation over restricted m values such that the transition between m and n belongs to α .

Since unidirectional transitions violate the microscopic reversibility, they should be excluded from evaluating EP; otherwise, the EP diverges. We denote the EPs for one time step excluding unidirectional transitions as

$$\Delta \tilde{\Sigma}^{(b)}(t_i) \equiv \sum_{n,m}^{(b)} M_{n,m}^{(b)}(t_i) P_m(t_i) \ln \frac{M_{n,m}^{(b)}(t_i) P_m(t_i)}{M_{m,n}^{(b)}(t_i) P_n(t_i)} \quad (25)$$

and

$$\Delta \Sigma^{(b)}(t_i) \equiv \sum_{n,m}^{(b)} M_{n,m}^{(b)}(t_i) P_m(t_i) \ln \frac{M_{n,m}^{(b)}(t_i) P_m(t_i)}{M_{m,n}^{(b)}(t_i) P_n(t_{i+1})}, \quad (26)$$

and we define two kinds of dynamical activities

$$A^{(\alpha)}(t_i) \equiv \sum_{m \neq n}^{(\alpha)} M_{n,m}^{(\alpha)}(t_i) P_m(t_i) \quad (27)$$

for $\alpha \in \{u, b\}$. Note that the dynamical activity for unidirectional transition can be written as

$$A^{(u)}(t_i) = \frac{1}{2} \sum_{m \neq n}^{(u)} |M_{n,m}^{(u)} P_m(t_i) - M_{m,n}^{(u)} P_n(t_i)|. \quad (28)$$

The triangle inequality leads to

$$\begin{aligned} & \sum_{\alpha=u,b} \sum_{m \neq n}^{(\alpha)} |M_{n,m}^{(\alpha)} P_m(t_i) - M_{m,n}^{(\alpha)} P_n(t_i)| \\ & \geq \sum_n \left| \sum_{\alpha=u,b} \sum_{m (\neq n)}^{(\alpha)} [M_{n,m}^{(\alpha)} P_m(t_i) - M_{m,n}^{(\alpha)} P_n(t_i)] \right| \\ & = \sum_n |P_n(t_{i+1}) - P_n(t_i)| = 2d_{i+1,i}. \end{aligned} \quad (29)$$

Using the relation

$$\begin{aligned} & \sum_{\alpha=u,b} \sum_{m \neq n}^{(\alpha)} |M_{n,m}^{(\alpha)} P_m(t_i) - M_{m,n}^{(\alpha)} P_n(t_i)| \\ & = \sum_{m \neq n}^{(b)} |M_{n,m}^{(b)} P_m(t_i) - M_{m,n}^{(b)} P_n(t_i)| + 2A^{(u)}(t_i), \end{aligned} \quad (30)$$

Eq. (29) is reexpressed as

$$\frac{A^{(b)}(t_i)}{2} \sum_{m \neq n}^{(b)} |Q_{n,m}^{(b)}(t_i) - Q_{m,n}^{(b)}(t_i)| \geq d_{i+1,i} - A^{(u)}(t_i), \quad (31)$$

where $Q_{n,m}^{(b)}(t_i) \equiv M_{n,m}^{(b)}(t_i) P_m(t_i) / A^{(b)}(t_i)$. Along with this inequality, by following a similar derivation procedure as presented in Eqs. (11), (12), and (16), we arrive at the stepwise speed limit for a system including unidirectional transitions as follows:

$$\tilde{\Sigma}^{(b)} \geq \sum_{i=0}^{N-1} A^{(b)}(t_i) h \left(\frac{d_{i+1,i} - A^{(u)}(t_i)}{A^{(b)}(t_i)} \right). \quad (32)$$

Note that Eq. (32) is valid only when $d_{i+1,i} - A^{(u)}(t_i) \geq 0$ for all t_i , since $h(x)$ is a monotonically increasing function only for $x \geq 0$.

Additionally, by applying Eqs. (17) and (19) to Eq. (32), we obtain the speed limit with unidirectional transitions as well, which is

$$\tilde{\Sigma}^{(b)} \geq A_{\text{tot}}^{(b)} h \left(\frac{d_{\text{TV}}[\mathbf{P}(t_{\text{F}}), \mathbf{P}(t_{\text{I}})] - A_{\text{tot}}^{(u)}}{A_{\text{tot}}^{(b)}} \right) \quad (33)$$

with $A_{\text{tot}}^{(\alpha)} = \sum_{i=0}^{N-1} A^{(\alpha)}(t_i)$. Similarly, Eq. (33) is valid when the argument of $h(x)$ is positive. Thus, if $A^{(u)}(t_i)$ is too large, Eq. (33) can be violated. Equations (32) and (33) clearly show that the bound is modified by the dynamical activities associated with both types of transitions. Since the contribution of unidirectional transitions is not included in $\tilde{\Sigma}^{(b)}$, the dynamical activity associated with unidirectional transitions is subtracted from the total variation distance, which tends to decrease the bound of $\tilde{\Sigma}^{(b)}$.

We note that there is a speed limit for a continuous-time process with unidirectional transitions in terms of a thermodynamic metric [15], different from the time-continuum limit of (33).

V. NUMERICAL VERIFICATION

In this section, we numerically verify our results through three examples: a one-time-step process of a two-state system, a cyclic process of a two-state system, and a relaxation process involving a unidirectional transition.

A. One-time-step process

The first example is a one-time-step evolution of a system with two states, labeled as 0 and 1. The energy gap between these states is denoted as E_1 . To determine the transition probabilities $M_{n,m}$ for a discrete-time process, we begin by examining a continuous-time relaxation process for the two-state system, which is in contact with a

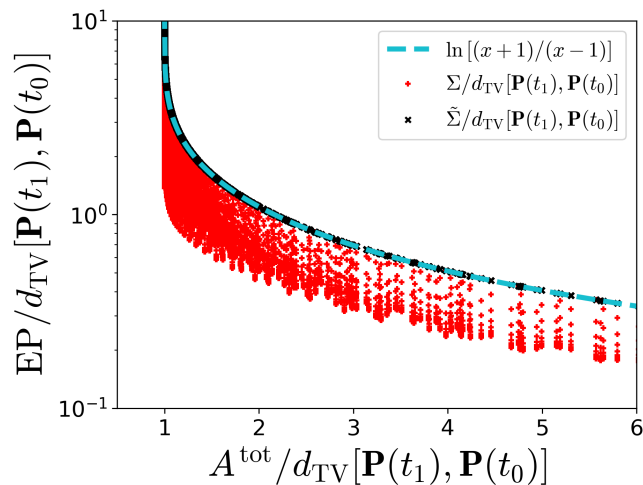


FIG. 1. Plot of EP versus total dynamical activity for one-time-step relaxation process of the two-state system presented in Sec. V A. Both the x and y axes are scaled by total variation distance. $+$ and \times symbols represent scaled time-backward EP and time-reversed EP, respectively. The cyan dashed line denotes the speed limit bound estimated from $h(x) = h_{\text{sym}}(x)$ function. The parameters used for this plot are as follows: $\mu = T = 1$, $0 \leq E_1 \leq 10$, $0 \leq \Delta t \leq 20$ and $0.001 \leq g \leq 0.99$.

thermal reservoir at temperature T . The master equation of this continuous-time dynamics is

$$\dot{\mathbf{P}}(t) = \mathbf{R} \cdot \mathbf{P}(t), \quad (34)$$

where the transition rates $R_{1,0} = \mu\gamma$ and $R_{0,1} = \mu(1-\gamma)$ follows the Arrhenius rule with $\gamma = e^{-E_1/T}/(1+e^{-E_1/T})$. The diagonal elements of \mathbf{R} are determined by $R_{0,0} = -R_{1,0}$ and $R_{1,1} = -R_{0,1}$ due to the normalization condition $\sum_n R_{n,m} = 0$. The formal solution of Eq. (34) is

$$\mathbf{P}(t_1) = e^{\mathbf{R}(t_1-t_0)} \cdot \mathbf{P}(t_0) \equiv \mathbf{M} \cdot \mathbf{P}(t_0), \quad (35)$$

where the transition probability matrix is given by

$$\mathbf{M} = \begin{pmatrix} 1 - \gamma(1 - e^{-\mu\Delta t}) & (1 - \gamma)(1 - e^{-\mu\Delta t}) \\ \gamma(1 - e^{-\mu\Delta t}) & \gamma + (1 - \gamma)e^{-\mu\Delta t} \end{pmatrix} \quad (36)$$

with the time interval $\Delta t = t_1 - t_0$. Equation (35) serves as the equation of motion for our discrete-time process.

Figure 1 shows the plot of time-reserved and time-backward EPs with respect to the total dynamical activity. Note that the x and y axes of the plot are scaled by the total variation distance. The parameters $N = T = \mu = 1$ are used for this plot. The initial probabilities are parameterized as $P_0(t_0) = g$ and $P_1(t_0) = 1 - g$. By choosing various values of g , E_1 and Δt , we evaluate the scaled EPs and A_{tot} . The plot demonstrates that time-reversed EP saturates to the speed limit bound estimated from $h(x) = h_{\text{sym}}(x)$. This verifies the saturation condition discussed in Sec. III C. On the other hand, time-backward EP violates the bound.

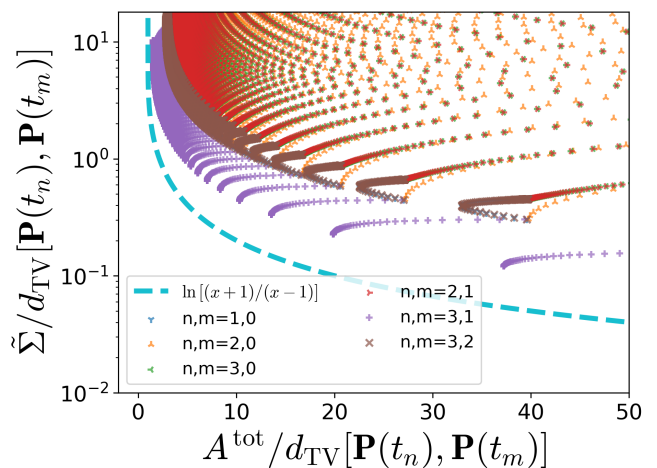


FIG. 2. Plot of time-reversed EP versus total dynamical activity for the cyclic steady-state process presented in Sec. V B. Both the x and y axes are scaled by total variation distance. The dashed line denotes the section speed limit using $h(x) = h_{\text{sym}}(x)$ function. Different symbols represent different choices of n and m for total variation distance $d_{\text{TV}}[\mathbf{P}(t_n), \mathbf{P}(t_m)]$. The parameters used for this plot are as follows: $\mu = T = 1$, $E_0 = 0$, $0.01 \leq \Delta E \leq 7$, and $0.01 \leq \Delta\tau \leq 7$.

B. Cyclic steady-state process

The second example is a two-state system under periodic driving over time. The time period is $\tau = 4\Delta t$, that is, a four-step process. The equation of motion for the system is the same as Eq. (35), with time-dependent energy gap $E_1(t)$: $E_1(t_0) = \Delta E$, $E_1(t_1) = 0$, $E_1(t_2) = -\Delta E$, and $E_1(t_3) = 0$.

To verify the section speed limit, we calculate the time-reversed EP and dynamical activity for the complete cycle, while also evaluating the total variation distance for all possible combinations of intermediate distributions at cyclic steady state. For this calculation, we set $\mu = T = 1$ and used various values of ΔE and $\Delta\tau$ within the range from 0.01 to 7. The calculation results are presented in Fig. 2. The figure illustrates that for all non-zero total variation distances, the section speed limit provides meaningful bounds on EP. Especially, $d_{\text{TV}}[\mathbf{P}(t_1), \mathbf{P}(t_3)]$ gives the tightest bound. This contrasts with the conventional speed limit, determined by the initial and final distributions, which yields a meaningless bound for a cyclic process. Thus, the results demonstrate the usefulness of the derived speed limit in EP estimation problem for a cyclic process.

C. System with unidirectional transition

The last example is a three-state model with one absorbing state indexed as 2. The equation of motion is given by

$$\mathbf{P}(t_{i+1}) = [\mathbf{M}^{(b)} + \mathbf{M}^{(u)}]\mathbf{P}(t_i), \quad (37)$$

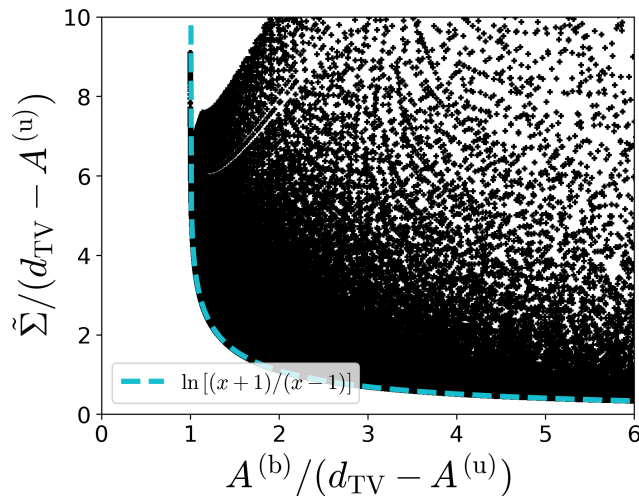


FIG. 3. Plot of time-reversed EP versus dynamical activity of bidirectional transitions for the one-time-step relaxation process of the system, including a unidirectional transition, as presented in Sec. V C. Both the x and y axes are scaled by $d_{TV}[\mathbf{P}(t_1), \mathbf{P}(t_0)] - A^{(u)}(t_0)$. The dashed line represents the speed limit for a system including unidirectional transitions, given by Eq. (33), using $h(x) = h_{\text{sym}}(x)$. The black dots denote calculation results obtained from various values of g , $M_{1,0}$, and $M_{0,1}$ within the range (0.01, 0.9) under the constraint $d_{TV}[\mathbf{P}(t_1), \mathbf{P}(t_0)] - A^{(u)}(t_0) > 0$.

where the transition probability matrix for bidirectional transitions is

$$\mathbf{M}^{(b)} = \begin{pmatrix} 1 - M_{10} & M_{01} & 0 \\ M_{10} & 1 - M_{01} - M_{21} & 0 \\ 0 & 0 & 1 \end{pmatrix} \quad (38)$$

and the transition probability matrix for a unidirectional transition is

$$\mathbf{M}^{(u)} = \begin{pmatrix} 0 & 0 & 0 \\ 0 & 0 & 0 \\ 0 & M_{21} & 0 \end{pmatrix}. \quad (39)$$

The initial condition is parameterized as $\mathbf{P}(t_0) = (g, 1 - g, 0)^T$, where g denotes the initial probability of being in state 0. Because there is no outgoing transitions from state 2, the system eventually relaxes to the absorbing state with $P_n(\infty) = \delta_{n,2}$.

We evaluate time-reversed EP and dynamical activity for the one-time-step relaxation process described by Eq. (37). The results are plotted in Fig. 3. The dashed line represents the bound of the speed limit for a system including unidirectional transitions, as given by Eq. (33), using $h(x) = h_{\text{sym}}(x)$. Data points indicate the results obtained from various values of g , $M_{1,0}$, and $M_{0,1}$

chosen within the range (0.01, 0.9) under the constraint $d_{TV}[\mathbf{P}(t_1), \mathbf{P}(t_0)] - A^{(u)}(t_0) > 0$. This example validates the speed limit for a system consisting of unidirectional transitions and demonstrates its tightness.

VI. CONCLUSIONS

We investigated the speed limits in discrete-time Markov chains. We found that time-reversed EP satisfies the speed limit in the same form as the conventional relation, while time-backward EP violates this bound. This contrasts with TUR: in a discrete-time process, the bound of time-reversed EP in TUR is exponentially suppressed or dependent on the minimum staying probability. Therefore, we anticipate that the discrete-time speed limit can provide a more efficient method for estimating EP in Markov chains compared to discrete-time TUR.

We also derived several variants of the conventional speed limit. The first is the stepwise speed limit which offers a bound in terms of distances between two consecutive probability distributions at all time steps. Second, we derived the section speed limit which is expressed solely by a single distance between any intermediate-time points. This relation is useful especially when only partial-time information on probability distributions is available. In addition, this relation can provide a non-trivial bound even in systems driven by a cyclic protocol and generally provides a tighter bound. Finally, we obtained a modified speed limit for systems with unidirectional transitions. This relation can be applied to various systems with absorbing states such as extinction dynamics and opinion dynamics.

Our derivation approaches are also applicable to continuous-time Markov processes, ensuring the validity of the derived relations in continuous-time processes. We believe that our findings will contribute to exploring thermodynamics in both discrete-time and continuous-time systems, where existing speed limits may not be applicable.

ACKNOWLEDGMENTS

This research was supported by the KIAS Individual Grant Nos. PG081802 (S.L.), and PG064902 (J.S.L.) at the Korea Institute for Advanced Study and an appointment to the JRG Program at the APCTP through the Science and Technology Promotion Fund and Lottery Fund of the Korean Government (J.-M.P.). This was also supported by the Korean Local Governments - Gyeongangbuk-do Province and Pohang City (J.-M.P.)

[1] U. Seifert, Phys. Rev. Lett. **95**, 040602 (2005).
[2] U. Seifert, Rep. Prog. Phys. **75**, 126001 (2012).

[3] C. Jarzynski, Phys. Rev. Lett. **78**, 2690 (1997).
[4] G. E. Crooks, Phys. Rev. E **60**, 2721 (1999).

- [5] M. Esposito and C. Van den Broeck, Phys. Rev. Lett. **104**, 090601 (2010).
- [6] C. Pérez-Espigares, A. B. Kolton, and J. Kurchan, Phys. Rev. E **85**, 031135 (2012).
- [7] R. E. Spinney and I. J. Ford, Phys. Rev. Lett. **108**, 170603 (2012).
- [8] H. K. Lee, C. Kwon, and H. Park, Phys. Rev. Lett. **110**, 050602 (2013).
- [9] D. Collin, F. Ritort, C. Jarzynski, S. B. Smith, I. Tinoco Jr, and C. Bustamante, Nature **437**, 231 (2005).
- [10] A. C. Barato and U. Seifert, Phys. Rev. Lett. **114**, 158101 (2015).
- [11] Y. Hasegawa and T. Van Vu, Phys. Rev. Lett. **123**, 110602 (2019).
- [12] J. M. Horowitz and T. R. Gingrich, Nat. Phys. **16**, 15 (2020).
- [13] T. Koyuk and U. Seifert, Phys. Rev. Lett. **125**, 260604 (2020).
- [14] K. Liu, Z. Gong, and M. Ueda, Phys. Rev. Lett. **125**, 140602 (2020).
- [15] D. Gupta and D. M. Busiello, Phys. Rev. E **102**, 062121 (2020).
- [16] T. Van Vu and Y. Hasegawa, Phys. Rev. Lett. **126**, 010601 (2021).
- [17] A. Pal, S. Reuveni, and S. Rahav, Phys. Rev. Res. **3**, 013273 (2021).
- [18] J. S. Lee, J.-M. Park, and H. Park, Phys. Rev. E **104**, L052102 (2021).
- [19] A. Pal, S. Reuveni, and S. Rahav, Phys. Rev. Res. **3**, L032034 (2021).
- [20] J.-M. Park and H. Park, Phys. Rev. Res. **3**, 043005 (2021).
- [21] A. Dechant and S.-i. Sasa, Phys. Rev. E **97**, 062101 (2018).
- [22] A. Dechant and S.-i. Sasa, Prod. Natl. Acad. Sci. **117**, 6430 (2020).
- [23] N. Shiraishi, K. Saito, and H. Tasaki, Phys. Rev. Lett. **117**, 190601 (2016).
- [24] P. Pietzonka and U. Seifert, Phys. Rev. Lett. **120**, 190602 (2018).
- [25] J. S. Lee, J.-M. Park, H.-M. Chun, J. Um, and H. Park, Phys. Rev. E **101**, 052132 (2020).
- [26] Y. Oh and Y. Baek, Phys. Rev. E **108**, 024602 (2023).
- [27] D. Hartich and A. Godec, Phys. Rev. Lett. **127**, 080601 (2021).
- [28] J. Li, J. M. Horowitz, T. R. Gingrich, and N. Fakhri, Nat. Commun. **10**, 1666 (2019).
- [29] D.-K. Kim, S. Lee, and H. Jeong, Phys. Rev. Res. **4**, 023051 (2022).
- [30] S. Otsubo, S. K. Manikandan, T. Sagawa, and S. Krishnamurthy, Commun. Phys. **5**, 11 (2022).
- [31] S. Lee, D.-K. Kim, J.-M. Park, W. K. Kim, H. Park, and J. S. Lee, Phys. Rev. Res. **5**, 013194 (2023).
- [32] E. Kwon and Y. Baek, arXiv preprint arXiv:2303.02901 (2023).
- [33] N. Shiraishi, K. Funo, and K. Saito, Phys. Rev. Lett. **121**, 070601 (2018).
- [34] J.-C. Delvenne and G. Falasco, arXiv preprint arXiv:2110.13050 (2021).
- [35] J. S. Lee, S. Lee, H. Kwon, and H. Park, Phys. Rev. Lett. **129**, 120603 (2022).
- [36] S. Ito and A. Dechant, Phys. Rev. X **10**, 021056 (2020).
- [37] A. Dechant, J. Phys. A **55**, 094001 (2022).
- [38] T. Van Vu and K. Saito, Phys. Rev. X **13**, 011013 (2023).
- [39] K. Proesmans, J. Ehrich, and J. Bechhoefer, Phys. Rev. E **102**, 032105 (2020).
- [40] E. Kwon, J.-M. Park, J. S. Lee, and Y. Baek, arXiv preprint arXiv:2311.01098 (2023).
- [41] T. Van Vu and K. Saito, Phys. Rev. A **109**, 042209 (2024).
- [42] N. G. Van Kampen, *Stochastic processes in physics and chemistry*, Vol. 1 (Elsevier, 1992).
- [43] K. Proesmans and C. Van den Broeck, EPL **119**, 20001 (2017).
- [44] A. M. Timpanaro, G. Guarnieri, J. Goold, and G. T. Landi, Phys. Rev. Lett. **123**, 090604 (2019).
- [45] M. Igarashi, arXiv preprint arXiv:2205.07214 (2022).
- [46] P. Gaspard, J. Stat. Phys. **117**, 599 (2004).
- [47] J. Lee, Phys. Rev. E **97**, 032110 (2018).
- [48] M. S. Pinsker, Information and information stability of random variables and processes (in russian), Moscow: Izv. Akad. Nauk (1960).
- [49] G. L. Gilardoni, An improvement on Vajda's inequality, in In and Out of Equilibrium 2, edited by Vlaslas Sidoravicius and Maria Eulália Vares (Birkhäuser Basel, Basel, 2008), pp. 299–304.